Decay Products of the S_3 State of the Oxygen-Evolving Complex of Photosystem II at Cryogenic Temperatures. Pathways to the Formation of the $S = {}^7/_2$ S_2 State Configuration†

Nikolaos Ioannidis* and Vasili Petrouleas*

Institute of Materials Science, NCSR "Demokritos", 153 10 Aghia Paraskevi Attikis, Greece

Received November 29, 2001; Revised Manuscript Received June 3, 2002

ABSTRACT: The water-oxidizing complex of photosystem II cycles through five oxidation states, denoted S_i ($i = 0-4$), during water oxidation to molecular oxygen, which appears at the (transient) S_4 state. The recent detection of bimodal EPR signals from the S_3 state [Matsukawa, T., Mino, H., Yoneda, D., Kawamori, A. (1999) *Biochemistry 38,* 4072−4077] has drawn significant attention to this critical state. An interesting property of the S_3 state is the sensitivity to near-IR (NIR) light excitation. Excitation of the S_3 state by near-IR light at cryogenic temperatures induces among other signals a derivative-shaped EPR signal at $g = 5$ [Ioannidis, N., and Petrouleas, V. (2000) *Biochemistry 3*9, 5246−5254]. The signal bears unexpected similarities to a signal observed earlier in samples that had undergone multiple turnovers and subsequently had been stored at 77 K for a week or longer [Nugent, J. H. A., Turconi, S., and Evans, M. C. W. (1997) *Biochemistry 3*6, 7086−7096]. Recently, both signals were assigned to an $S = {}^7/_2$ configuration of the Mn cluster [Sanakis, Y., Ioannidis, N., Sioros, G., and Petrouleas, V. (2001) *J. Am. Chem. Soc. 123*, 10766−10767]. In the present study, we employ bimodal EPR spectroscopy to investigate the pathways of formation of this unusual state. The following observations are made: (i) The $g = 5$ signal evolves in apparent correlation with the diminution of the S_3 state signals during the slow (tens of hours to several days range) charge recombination of S_3 with Q_A^- at 77 K. The tyrosyl radical $D^\bullet$ competes with S_3 for recombination with Q_A^-, the functional redox couple at cryogenic temperatures inferred to be $D^\bullet/D^-$. Transfer to −50 °C and above results in the relaxation of the $g = 5$ to the multiline and $g = 4.1$ signals of the normal S_2 state. (ii) The transition of S_3 to the state responsible for the $g = 5$ signal can be reversed by visible light illumination directly at −30 °C or by illumination at 4.2 K followed by brief (2 min) transfer to −50 °C in the dark. The latter step is required in order to overcome an apparent thermal activation barrier (charge recombination appears to be faster than forward electron transfer at 4.2 K). (iii) The "$g = 5$" state can be reached in a few tens of minutes at 4.2 K by near-IR light excitation of the S_3 state. This effect is attributed to the transfer of the positive hole from the Mn cluster to a radical (probably tyr Z), which recombines much faster than the Mn cluster with Q_A^-. (iv) The above properties strongly support the assignment of the configuration responsible for the $g = 5$ signal to a modified S_2 state, denoted S_2'. Evidence supporting the assignment of the S_2' to a proton-deficient S_2 configuration is provided by the observation that the spectrum of S_2 at pH 8.1 (obtained by illumination of the S_1 state at −30 °C) contains a $g = 5$ contribution.

Photosystem II, PSII[1], catalyzes the light-induced oxidation of water to molecular oxygen. The site for this unique reaction is the so-called oxygen-evolving complex, OEC. OEC is the electron donor of PS II and cycles through five oxidation states S_0... S_4 during light-induced sequential electron flow (for reviews, see *1-6*).

EPR spectroscopy has played an important role in the study of the oxygen-evolving complex. EPR signals have now been detected from all S states, with the exception of the metastable S_4 state. The S_0 state is characterized by a $S = {}^1/_2$ signal with weak hyperfine lines extending over a width of approximately 2800 G (*7−9*). The S_1 state is characterized by an integer spin signal at $g = 4.8$ with no resolved hyperfine structure (*10, 11*) or by an alternative multiline signal centered at $g = 12$ (*12*), both detected by parallel mode EPR. The S_2 state is characterized by the extensively studied

† This work was supported in part by the EC Grant ERBFM-RXCT980214 and by the Greek Secretariat of Research and Technology (PENED 99ED75).

* Corresponding authors. V. Petrouleas: tel, +301 650-3344; fax, +301 6519430; e-mail, vpetr@ims.demokritos.gr. N. Ioannidis: tel, +301 650-3312; fax, +301 6519430; e-mail, nioannid@ims.demokritos.gr.

[1] Abbreviations: PSII, Photosystem II; OEC, oxygen-evolving complex; WOC, water-oxidizing complex; S states S_0...S_4 oxidation states of the water-oxidizing complex; tyr Z or Y_Z and tyr D or Y_D, the fast and slow tyrosine electron donors of PSII; signal II, the unperturbed EPR spectrum of either of the two tyrosines, a measure of oxidized tyr D under the present conditions; broad or split $g \sim 2$ signal, a broadened radical signal assigned to Tyr Z; Q_A and Q_B, the primary and secondary plastoquinone electron acceptors of PSII; BBY membranes, thylakoid membrane fragments enriched in PSII; MES, 2-[N-Morpholineethanesulfonic acid]; chl, chlorophyll; EtOH, ethanol; MeOH, methanol; cw EPR, continuous wave electron paramagnetic resonance; NIR light, near-infrared light.

10.1021/bi0159938 CCC: $22.00
Published on Web 07/02/2002

multiline signal ($S = {}^1/_2$) at $g = 2$ (*13*) and the alternative $g = 4.1$ signal ($S \geq {}^3/_2$) (*14*, *15*). An unusual and interesting property of the S_2 state is the sensitivity to near-infrared light, NIR. The multiline signal can be converted to the $g = 4.1$ signal via an intermediate $S \geq {}^5/_2$ state ($g = 10, 6$) by NIR illumination at temperatures greater than 60 K (*16*, *17*).

Recently, low field EPR signals in both perpendicular and parallel mode EPR were detected from the S_3 state (*18*). The observations were subsequently confirmed, and interestingly a sensitivity of this state to NIR illumination was observed (*19*). These observations, which were made in plant material, were reproduced in a cyanobacterial preparation (*20*).

NIR-light excitation of the S_3 state produces, in addition to other signals that appear to be associated with excited-state configurations of S_3 (*21*), a derivative-shaped EPR signal at $g = 5$ (*19*). This signal bears unexpected similarities to a signal observed earlier by Nugent and co-workers in samples that had undergone multiple turnovers above S_1 and subsequently had been stored at 77 K for a week or longer (*22*). In a recent communication, the $g = 5$ signal was assigned to an $S = {}^7/_2$ configuration of the S_2 state (*23*). The nearly isotropic $g = 5$ resonance originates from the "$\pm 3/2$" doublet of the $S = {}^7/_2$ manifold. A weaker resonance at around $g = 2.9$, whose position and intensity vary strongly with slight changes in the crystal-field parameters, results from the "$\pm 1/2$" doublet.

In the present study, we correlate the $g = 5$ signal formation with the decay of the S_3-state signals and furthermore compare the two seemingly different mechanisms (long-term incubation at 77 K vs NIR excitation at liquid-helium temperatures), which, apparently, result in the same modified S_2 configuration. Evidence in support of the earlier proposal that this modified S_2 configuration is deprotonated (*22*), is provided by the observation that a $g = 5$ signal is produced directly by illumination of the S_1 state, at -30 °C and alkaline pH.

MATERIALS AND METHODS

PSII-enriched thylakoid membranes were isolated from market spinach by standard procedures (*24*, *25*) with some modifications. Samples for EPR measurements were suspended in 0.4 M sucrose, 15 mM NaCl, 40 mM MES, pH 6.5, at 6−8 mg chl/mL and stored in liquid nitrogen until use.

Advancement to the S_3 state was achieved essentially as previously described (*19*). Samples (at 1 mg of chl/ml) were incubated with 2 mM ferricyanide at 4 °C, for 30 min, to oxidize the nonheme iron. The oxidant was subsequently removed by 3−4 wash steps in ferricyanide-free buffer by centrifugation at 35 000*g*. The final pellet was resuspended with oxidant-free buffer supplemented with 0.2 mM atrazine. The illumination procedure was as follows. BBY samples with preoxidized nonheme iron, initially kept at 4 °C in darkness, were rapidly transferred into a −30 °C precooled acetone bath under illumination, illuminated for 3 min, and finally placed in liquid nitrogen. For this purpose, white light from a 340 W projection lamp, filtered through a solution of $CuSO_4$, was used.

This procedure yielded approximately 50−60% S_3 and 50−40% S_2 state. The main contributions to the S_2 state presumably arose from centers in which the iron was not initially oxidized and from a fraction of centers in which the S_3 state was reduced during illumination by Y_D. These centers should have Q_A singly reduced. In addition, a third contribution, representing a small fraction of S_2 centers with Q_A oxidized, presumably arose from the S_3/Q_A^- recombination during the illumination/freezing period.

Signal II, a measure of $Y_D^\bullet$ in the present experiments, was monitored during all steps in the various experiments, and reference is made to its magnitude without showing the spectra, as they are trivial. Approximate normalization of signal II was done by assuming that the level of the signal at the end of the experiments and, following the full decay of S_3 and S_2 at about 15 °C, represented approximately 100% of the centers. This is a reasonable assumption considering that two electrons are transferred to the acceptor side—one to Q_A and one to Fe(III)—during formation of the S_3 state, but only Q_A^- is available for charge recombination (the oxidized iron is a stable electron acceptor). Thus, Y_D is the main alternative reductant of the excited S states (*26*). This must be added to the fact that a significant portion of this tyrosine is oxidized before the experiments (unless special precautions are taken) (*27*).

Excitation of the S_3 state by near-infrared light (NIR) was performed at 4.2 K. The projection lamp was filtered in this case by a 3 mm RG715 SCHOTT filter immersed in water. Illumination with white light was done in the same manner, but the projector light was filtered by a 3 mm BG-39 SCHOTT filter immersed in a $CuSO_4$ solution. The duration of illuminations was, unless otherwise stated, 3 min intermittently in 15 s intervals.

At the end of experiments, samples were dark adapted for typically 60 min at 4 °C, or 30 min at 15 °C, to relax to the S_1 state. The resulting EPR spectrum was used as a reference and was subtracted from all other spectra in order to eliminate background contributions due to oxidized cyt b_{559} and impurities. Following the dark adaptation period, samples were illuminated again at −30 °C in order to obtain the maximum S_2 state population.

The S_1-to-S_2 advancement at alkaline pH was performed as follows. PS II enriched membranes were centrifuged at 35 000*g* and resuspended twice in a buffer containing 0.4 M sucrose, 15 mM NaCl, 1 mM MES, pH 6.5. In the second resuspension step, the buffer was supplemented with 0.2 mM atrazine. Samples were illuminated at −30 °C for 2 min, and the S_2 state (pH 6.5) control spectra were recorded. The samples were subsequently allowed to decay to the S_1 state by dark adaptation at 15 °C, and the pH was raised to approximately 8 (measured at the end of the experiments) by the addition of 40 mM final concentration Tricine from a stock solution of 0.5 M, pH 8.5. After mixing (<30 s), the samples were either frozen immediately or allowed to equilibrate for up to 30 min at 15 °C (no significant differences were observed among the samples), and the alkaline S_1 spectra were recorded. The S_2 state spectrum was obtained subsequently after illumination at −30 °C.

EPR measurements were performed with a Bruker ER-200D-SRC spectrometer interfaced to a personal computer and equipped with an Oxford ESR 900 cryostat, an Anritsu MF76A frequency counter, and a Bruker 035M NMR gaussmeter. Where not specified, the perpendicular 4102ST cavity was used, and the microwave frequency was 9.41 GHz with 4 mm and 9.39 GHz with 5 mm tubes. The spectra

obtained with the standard cavity are the average of 2−4 scans. Tubes of 5 mm were exclusively used with the dual mode cavity, 4116 DM, and 4 or 10 accumulations were done in the perpendicular or the parallel mode, respectively. The microwave frequency was 9.60 GHz in the perpendicular and 9.31 GHz in the parallel mode.

RESULTS AND DISCUSSION

Decay of the S_3 State at 77 K. Nugent et al. (*22*) reported a signal at about $g = 5$ in samples that had undergone multiple turnovers above the S_1 state and subsequently had been stored at 77 K for more than 1 week. The signal was assigned to a modified S_2 state, which accumulated during the decay of the S_3 state at 77 K; however, alternative possibilities, e.g., assignment of the signal to a modified form of the oxidized nonheme iron, could not be excluded. In view of the recent detection of EPR signals from the S_3 state (*19*), we have examined the time course of its decay and the concomitant evolution of other signals at 77 K. This is depicted in Figure 1. A sample with the nonheme iron preoxidized was illuminated as described in the Materials and methods section and thus advanced to the S_3 state, trace a. Then, the sample was incubated at 77 K in the dark, and spectra were collected after 17 h (trace b), 36 h (trace c), and 172 h (trace d). The following observations can be made. During incubation at 77K, the signals assigned to the S_3 state ($g = 10$), the S_2 state (multiline and $g = 4.1$), and the Q_A^-Fe(II) complex decrease gradually; in addition, signal II (a measure of oxidized Y_D under the present conditions, see also Materials and Methods) decreases (see later in this section) due to recombination with Q_A^- (*28*, *22*).

The above changes are accompanied by the gradual formation of a signal at $g = 5$ (apparently the same signal reported by Nugent et al., *22*). The intensity of the signal becomes maximal after incubation of the S_3 state at 77 K for about 1 week (Figure 1d). The signal is more pronounced at 4.2 K but at 11 K becomes significantly weaker. Small contributions from the $g = 4.1$ signal (S_2 state) distort somewhat its shape, particularly at 11 K (at 4.2 K the S_2 multiline and $g = 4.1$ signals are relatively smaller due to microwave power saturation). Incubation of samples at temperatures between 77 and 180 K, following incubation at 77 K for a few days, results in no significant changes except for a slight narrowing of the $g = 5$ signal (separate experiment not shown).

Warming of the sample in Figure 1d to −80 °C for 2 min causes a 30% decrease of the $g = 5$ signal and subsequent warming to −50 °C for another 2 min, Figure 1e, results in an almost complete loss of the $g = 5$ signal and a decrease of the $g = 10$ signal. A significant enhancement of the S_2 multiline and $g = 4.1$ signals,[2] as well as an increase in the signal II size (see later in this section) accompanies the last changes. Signal II reaches its maximum size (100%, see Materials and Methods) following a subsequent 30 min dark adaptation at 15 °C.

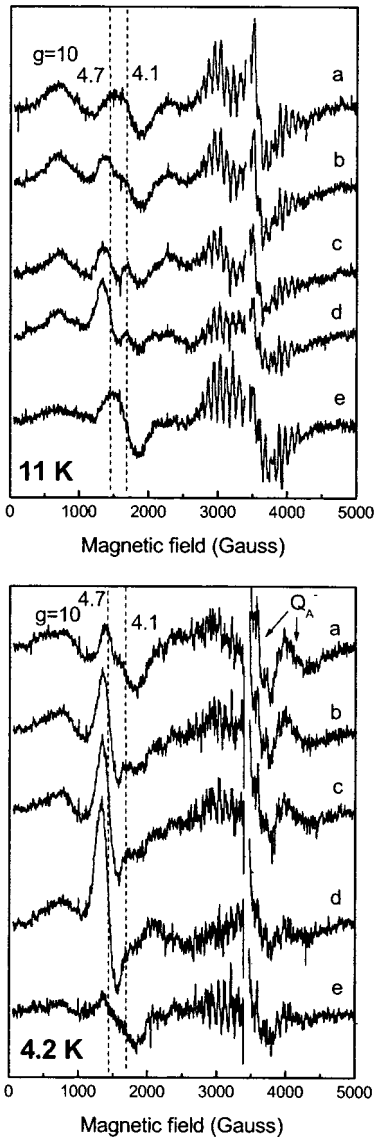

FIGURE 1: Time-dependent evolution of the $g = 5$ signal and diminution of the $g = 10$ signal during incubation of the S_3 state at 77 K. Spectrum a represents the S_3 state as prepared. Spectra b−d were recorded after 17, 36, and 172 h, respectively, of incubation time of the sample in trace a at 77 K. Finally, the sample was transferred to −80 °C for 2 min and subsequently to −50 °C for 2 min, spectrum e. All spectra are difference traces obtained after subtraction of the final dark-adapted spectrum as described in the Materials and Methods section. EPR conditions: temperature as indicated, microwave frequency 9.59 GHz, microwave power 35 mW, modulation amplitude 10 G, modulation frequency 100 kHz.

The S_3 decay has also been examined by parallel-mode EPR. Figure 2 shows the initial level of the S_3 signal (peak at $g = 17$) and the level of the signal after 82 h of incubation at 77 K. A significant decay of the S_3 signal is observed in agreement with the perpendicular-mode experiment of Figure 1.

The results of three experiments similar to those of Figures 1 and 2 are summarized in the diagrams of Figure 3, where the amplitude of the signals is plotted against incubation time at 77 K. The advancement to the S_3 state is taken as time zero, while the amplitudes of the various signals are normalized to the percentage of PSII centers they represent (see Materials and Methods). The calculation of the S_2 state fraction was based on the amplitude of the multiline signal,

[2] We confirmed in a separate experiment, using the standard cavity, the observation of Nugent et al. (*22*) that the restored S_2 multiline form at −80 °C is slightly different than the form obtained by illumination of S_1 samples at the same temperature. Changes in the $g = 4.1$ signal could not be positively detected due to interference from the $g = 5$ signal.

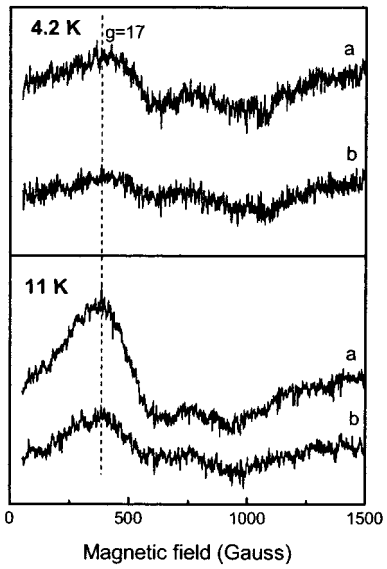

FIGURE 2: Decay of the S_3-state parallel-mode spectrum during prolonged storage at 77 K. Spectra, at the indicated temperatures, were recorded (a) immediately after the formation of the S_3 state and (b) after a subsequent 82 h incubation at 77 K. EPR conditions: microwave frequency 9.30 GHz, microwave power 8.2 mW at 4.2 K and 129 mW at 11 K, modulation amplitude 10 G, modulation frequency 100 kHz.

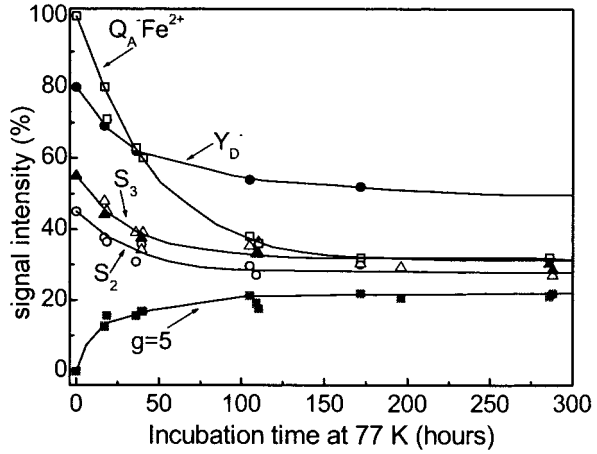

FIGURE 3: Time course of changes observed in the amplitude of various signals affected by the prolonged incubation of the S_3 state at 77 K. Filled squares, the $g = 5$ signal (modified S_2 state); open circles, the multiline signal (normal S_2 state); open triangles, the $g = 10$ signal (S_3 state, perpendicular mode); filled triangles, the $g = 17$ signal (S_3 state, parallel mode); filled circles, signal II slow ($Y_D^\bullet$); open squares, the Q_A^- semiquinone radical signal. Data points from three different experiments are pooled. The normalization of the signal amplitudes was done as described in the Materials and Methods section.

since the $g = 4.1$ signal is distorted by contributions from the $g = 5$ signal. Different symbols are used for the perpendicular-mode ($g = 10$, open triangles) and parallel-mode ($g = 17$, filled triangles) signals of the S_3 state, but it is reassuring to note that the decay traces coincide within experimental error. The following general remarks can be made comparing the intensity losses of the various signals. The $Q_A^-Fe^{2+}$ signal decreases by about 70%, presumably due to charge recombination with $Y_D^\bullet$ (*22*) in 28% of the centers and S_2 in 15% of the centers (these are centers where S_2 and Q_A^- coexist, see Materials and Methods). The remaining fraction is consistently accounted for by the 25% decay of S_3. These assignments are supported by the considerations below.

The $g = 5$ signal in Figure 1 is undoubtedly the same signal that has been reported by Nugent et al. (*22*). In the present case, atrazine restricts sample advancement beyond the S_3 state. In the absence of atrazine, both the size of the initial S_3 signal and the $g = 5$ signal that developed during 15 days of storage at 77 K were smaller compared to the control sample that contained the inhibitor atrazine (spectra not shown). On the other hand, we have confirmed the observations of Nugent et al. (*22*) that, samples poised at the S_2 state did not develop the $g = 5$ signal on storage at 77 K. In Figure 3a, correlation exists between the decay of the S_3 signals and the evolution of the $g = 5$ signal. The S_3-state EPR signals are indicative of an even number of electrons in this state. The $g = 5$ signal on the other hand has been assigned to a half-integer spin, $S = {}^7/_2$ (*23*), indicative of a configuration with an odd number of electrons. The most reasonable interpretation of the above results is that the evolution of the $g = 5$ signal is due to the reduction of the S_3 state at 77 K by one electron (due to charge recombination with Q_A^- as was assumed above). At elevated temperatures (−50 °C), the $g = 5$ signal is converted to the normal S_2 multiline and $g = 4.1$ signals (Figure 1e, see also ref *22*). Hence, the $g = 5$ signal is assigned to a modified S_2 configuration (we will subsequently call it S_2'), as was originally suggested (*22*). This interpretation is strongly supported by the fact that the decay of the S_3 state is reversed by white-light illumination (see below).

It is notable that the S_3 state does not decay fully at cryogenic temperatures, Figure 3. A nondecaying fraction of S_3 is observed even after very long incubation at 77 K (see also *21*). The results of Figure 3 indicate that $Y_D^\bullet$ is reduced concomitantly to the decay of the S_3 state. Presumably, $Y_D^\bullet$ and the S_3 state, which coexist in a significant fraction of centers, compete for charge recombination with Q_A^-, although direct redox exchange between $Y_D^\bullet$ and S_3 is also expected. It is reasonable to assume that during prolonged incubation at 77 K redox equilibrium is established between the Mn cluster and Y_D. There is general consensus that at ambient temperatures, Y_D is neutral in both the oxidized and the reduced form (for a recent review, see ref *29*). At cryogenic temperatures, exchange of a proton between this tyrosine and its surroundings is probably prohibited. This is suggested by the fact that Y_D, when frozen to cryogenic temperatures in the neutral-reduced state, does not function as a low temperature donor. However, when frozen in the oxidized state, $Y_D^\bullet$, is slowly reduced at 77 K by charge recombination with Q_A^- to the nonprotonated form, Y_D^-, and then becomes a very efficient electron donor at cryogenic temperatures. Illumination, in this case, with visible light at temperatures as low as 4.2 K, results readily in charge separation between Y_D^- and Q_A (*22*, *21*). The above observations can be rationalized if we assume that the functioning redox couple at 77 K is $Y_D^\bullet/Y_D^-$. It is possible that the two couples, $Y_D^\bullet/Y_D^-$ and S_3/S_2 ($g = 5$) have similar redox potentials.

A brief comment should be also made about the annealing step to −50 °C (Figure 1e). Recombination with Q_A^- is slower than the 2 min interval at this temperature (see next section), but Tyr D is expected to act as a rapid reductant of S_3 and S_2 in those centers were the reduced tyrosine (formed

mainly during the prolonged incubation at 77 K, Figure 3) coexists with either of the two states (*28*, *30*, *31*). As the $g = 5$ signal converts to the S_2 multiline and $g = 4.1$ forms, the net effect of the 2 min incubation at −50 °C, Figure 1e, is a decrease of the S_3 signals, and an enhancement of the S_2 signals. In addition, the oxidized fraction of tyr D is approximately restored to its level in Figure 1a. It should be noted that the decay of S_3 and S_2 at −50 °C is slow when Y_D is oxidized (see below). It has been also observed that the conversion of the $g = 5$ to the multiline and $g = 4.1$ signals is independent of the redox state of Y_D.

Decay of the S_3 State at Elevated Temperatures. It was noted above that no new signals develop during the incubation of the $g = 5$ containing samples at temperatures between 77 and 180 K, while at −50 °C the $g = 5$ signal relaxes within a few minutes to the S_2 multiline and $g = 4.1$ signals (see, however, footnote 2). On the other hand, we could not find a convenient temperature higher than 77 K that accelerated the reduction rate of the S_3 state to the $g = 5$ configuration. Most likely the decay of the $g = 5$ signal at elevated temperatures is faster than its production. At ca. 170 K, the $t_{1/2}$ for the decay of the S_3 state signal at $g = 10$ is longer than 8 h, while the $g = 5$ decays with an approximately halftime of a few hours. At −50 °C, the approximate halftime for the decay of S_3, due to recombination with Q_A^-, (samples with Y_D fully oxidized) is 30 min, while the $g = 5$ signal decays fully within 2 min. The decay products of the S_3 state at −50 °C are the S_2 multiline and $g = 4.1$ signals, at relative ratios approximately comparable to the native S_2 state. A typical sequence of events describing the decay of the S_3 state at elevated temperatures is exemplified by an experiment performed at −30 °C (Figure 4).

Following the initial population of the S_3 state (uppermost spectrum), spectra were collected after various time periods of incubation at −30 °C. At the end of the incubation period at −30 °C and after 30 min of additional dark adaptation at 15 °C—this allowed for the complete decay to the S_1 state—the sample was illuminated at 200 K, and the spectrum of the S_2 state was recorded as a reference. By comparison with the latter spectrum and assuming that the S_3 and S_2 are the main states occupied, the starting populations of the S_3 and S_2 states in Figure 4 are estimated at approximately 60% and 40% respectively. During incubation at −30 °C, the S_3 state signal at $g = 10$ declines continuously, but no clear buildup of the S_2 multiline or $g = 4.1$ signals is evident. It is clear, however, that the decline of the S_2 signals is significantly slower. The data are difficult to interpret quantitatively. A simple qualitative explanation would be that the initial S_3 and S_2 fractions recombine with Q_A^- with similar rate constants, while the fraction of S_2 resulting from the decay of S_3 is reduced more slowly by alternative reductants.

We have also examined a simpler case for comparison. In the presence of 5% (v/v) methanol, the S_2 state is represented by the multiline signal only (*32*). It was also noted in our earlier study (*19*) that no S_3 signals could be detected in the presence of methanol—occupation of this state was inferred by the diminished amplitude of the multiline signal—and no sensitivity to NIR light was observed. Thus, in an experiment similar to that of Figure 4, we examined the decay of the S_3 state in the presence of methanol (not shown). In this case, we did find a clear transient increase

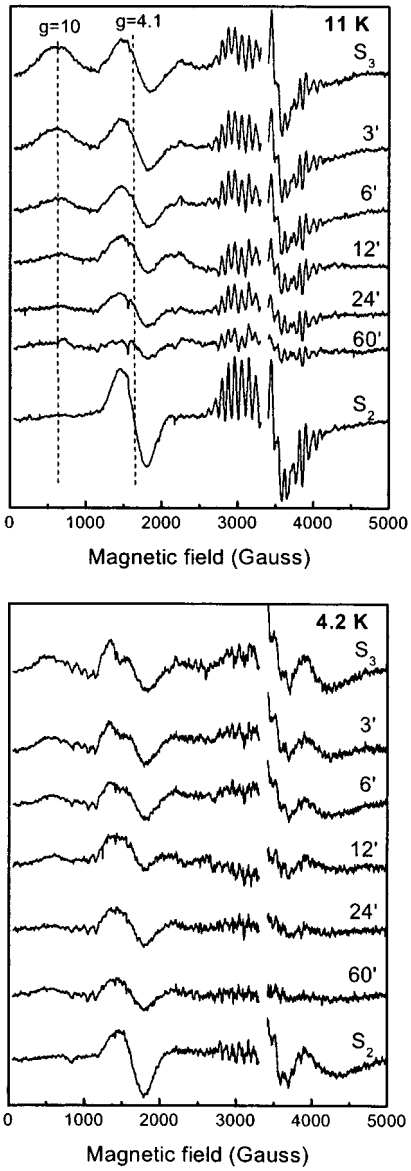

FIGURE 4: Decay of the S_3 state at −30 °C. Spectra labeled S_3 were recorded immediately after excitation to the S_3 state, and subsequent spectra were collected after incubation at −30 °C for the indicated time periods. The bottom spectrum represents the maximal intensity of the S_2 state. Difference spectra were obtained by subtraction of the dark-adapted spectrum obtained at the end of the measurements (see Materials and Methods). EPR conditions: temperature as indicated, microwave frequency 9.39 GHz, microwave power 35 mW, modulation amplitude 25 G, modulation frequency 100 kHz.

of the S_2 state multiline, which declined at longer times. A gradual decay of Q_A^- was observed in parallel.

The data on the $S_3Q_A^-$ recombination rate are scarce (*33*, *34*), but it is usually assumed that it is similar to that of the $S_2Q_A^-$ recombination. This is approximately 1 s at room temperature (*33*, *34*) and slows down to a $t_{1/2}$ of ca. 5 min at −25 °C (*35*, *36*). This estimate is supported by the decay rate of the $g = 10$ (S_3) and the $Q_A^-Fe^{2+}$ signals in Figure 4. In this experiment, the starting population of the S_3 state is higher than that of the S_2 state. If the decay process of the $g = 10$ signal to the multiline and $g = 4.1$ signals is first-order, one will expect, under these conditions, a transient built up of the S_2 signals, which is indeed observed in the presence of methanol (not shown). The absence of a transient

increase of the S_2 signals in Figure 4 may indicate a slow conversion to the conformations that produce the S_2 signals (see also ref *2*). Alternatively, the $S_2Q_A^-$ recombination rate may be somewhat faster than that of the $S_3Q_A^-$ in the untreated sample and slower in the MeOH treated one.

Recovery of the S_3 State, Following Its Decay, by Visible Light Illumination. The main states generated by the procedure used to form the S_3 state are $S_3Q_A^-$ and $S_2Q_A^-$ (see Materials and Methods). Charge recombination at −30 °C or lower (as described in the previous section) should produce the S_2Q_A and S_1Q_A states, respectively. Provided that the incubation at the elevated temperatures is not prolonged (that would lead to the slow reduction of S_2Q_A to S_1Q_A), illumination at −30 °C should induce charge separation and restore the initial states. This has been readily confirmed with samples advanced to the S_3 state and subsequently incubated at −50 °C long enough for charge recombination to occur. Since the $g = 5$ configuration is assigned to a modified S_2, S_2', a similar behavior should be exhibited by samples where the S_3 decayed after prolonged incubation at 77 K. This is demonstrated by the following two experiments.

In an experiment similar to Figure 1, a sample poised in the S_3 state, Figure 5a, was incubated at 77 K for 11 days until the $g = 10$ signal decreased considerably and a pronounced $g = 5$ signal developed, Figure 5b. The sample was subsequently incubated at −50 °C for 2 min, Figure 5c (a treatment similar to Figure 1e). Notable is the significant decrease of the $Q_A^-Fe^{2+}$ signal in traces b and c of Figure 5, indicating that charge recombination has occurred in the largest fraction of centers. As discussed in the first section, the initial level of tyr $D^\bullet$ is approximately restored at −50 °C; therefore, recombination must have occurred at the expense of the S_3 and S_2 states at this final stage. Assuming roughly equal initial populations of $S_2Q_A^-$ and $S_3Q_A^-$, the spectra of Figure 5c consist mainly of approximately equal populations of S_1Q_A and S_2Q_A (in addition to small portions of not recombined $S_2Q_A^-$ and $S_3Q_A^-$). Illumination at −30 °C, Figure 5d, clearly restores the starting population of states.

In the discussion related to Figures 1−3, it was concluded that the one-electron reduction of the S_3 state at 77 K gives rise to the S_2' state (characterized by the $g = 5$ signal). It is reasonable to expect that white-light illumination of the latter state at cryogenic temperatures will result in the formation of the initial S_3 state. The fact that this is possible has been implied by the experiments of Nugent et al. (*22*). These authors used samples which developed the $g = 5$ signal and noticed the induction of charge separation upon illumination at liquid helium temperatures. This charge separated couple recombined when stored at liquid helium temperatures, whereas at temperatures above 77 K, it was stabilized. Accordingly, the advancement of the $g = 5$ configuration of the Mn cluster to a higher oxidation state appeared to have an activation barrier below liquid nitrogen temperatures. Figure 6 repeats in a somewhat modified form the original experiment of Nugent et al. with the added advantage of knowing now the signature of the S_3 state. The experiment was followed by both perpendicular and parallel − mode EPR. Spectrum a shows the S_3 state as prepared. Spectrum b was recorded after several weeks of incubation at 77 K. It can be seen that the intensity of the S_3 signals, i.e., at $g = 10$ in perpendicular mode and $g = 17$ in parallel mode, is considerably diminished while a strong signal at $g = 5$ has appeared. Evident also is the great diminution of the Q_A^-Fe(II) signal. Visible-light illumination at 4.2 K of the sample, followed immediately by transfer to −50 °C, spectrum c (see ref *21* for the intermediates of this experiment), restores the Q_A^-Fe(II) signal to a high extent and causes the formation of a substantial amount of the S_3 state, as evidenced by the reformation of the $g = 10$ and 17 signals.

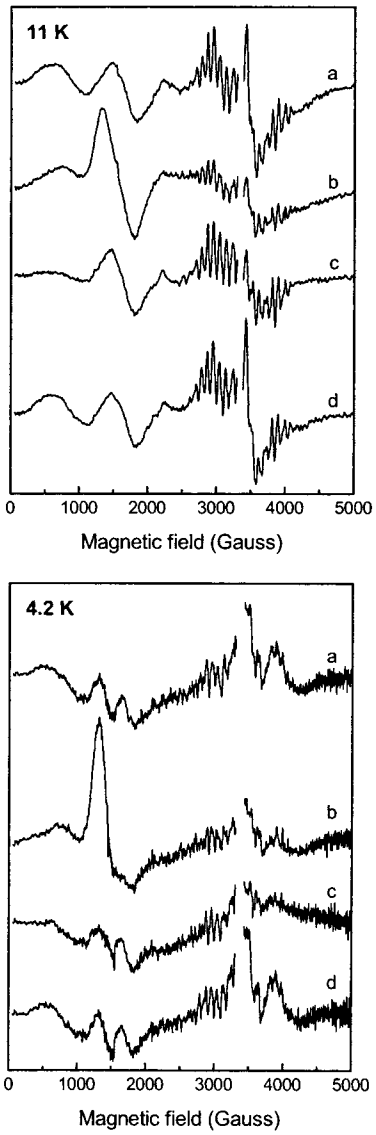

FIGURE 5: Recovery of the S_3 state, following its decay at 77 K, by visible light illumination at −30 °C. Spectra were recorded at 11 and 4.2 K after the following successive treatments of the same sample. (a) The S_3 state as prepared. (b) Incubation at 77 K for 11 days. (c) Warming to −50 °C for 2 min. (d) Illumination at −30 °C for 3 min. Difference spectra were obtained by subtraction of the dark adapted spectrum as described in the Materials and Methods. EPR settings are the same as those in Figure 4.

Clearly, the efficiency of the experiment of Figure 6 cannot be as high as of the one in Figure 5. In Figure 5, reduction of S_3 by tyr D at − 50 °C increased the fraction that had decayed to S_2 by the previous storage at 77 K. Furthermore, the illumination at −30 °C is far more efficient in producing charge separation than the illumination at liquid-helium temperatures. Nevertheless, recovery of the S_3 state by the unusual protocol of Figure 6 is clearly demonstrated.

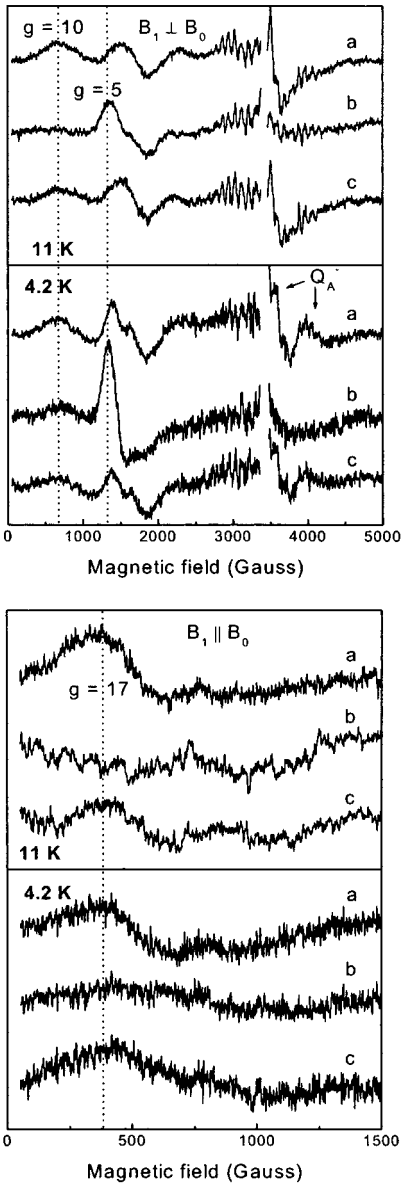

FIGURE 6: Recovery of the S_3 state, following its decay at 77 K, by visible light illumination at 4.2 K. Spectra at perpendicular and parallel modes were recorded after the following successive treatments of the same sample. (a) The S_3 state as prepared. (b) Incubation at 77 K for several weeks. (c) Illumination at 4.2 K for 3 min, immediately followed by transfer to −50 °C for 2 min. Difference spectra were obtained by subtraction of the dark adapted spectrum as described in the Materials and Methods section. Experimental conditions were the same as those in Figure 1 for the perpendicular-mode panels and as those in Figure 2 for the parallel-mode panels. Recording temperatures as indicated.

NIR Excitation of the S_3 State Accelerates Charge Recombination. The NIR excitation at 50 K of the S_3 state in (*19*) produced, in addition to other signals that appear to be associated with excited-state configurations of S_3 (*21*), a $g = 5$ signal, which shows notable similarities to the signal in Figure 1 produced slowly during storage of the S_3 state at 77 K. It was noted during the present studies that the changes induced by the NIR-light excitation of the S_3 state at about 50 K can be resolved better if the NIR-light excitation is performed at 4.2 K. A systematic study is presented in the accompanying paper (*21*). Here we focus on the formation of the $g = 5$ signal.

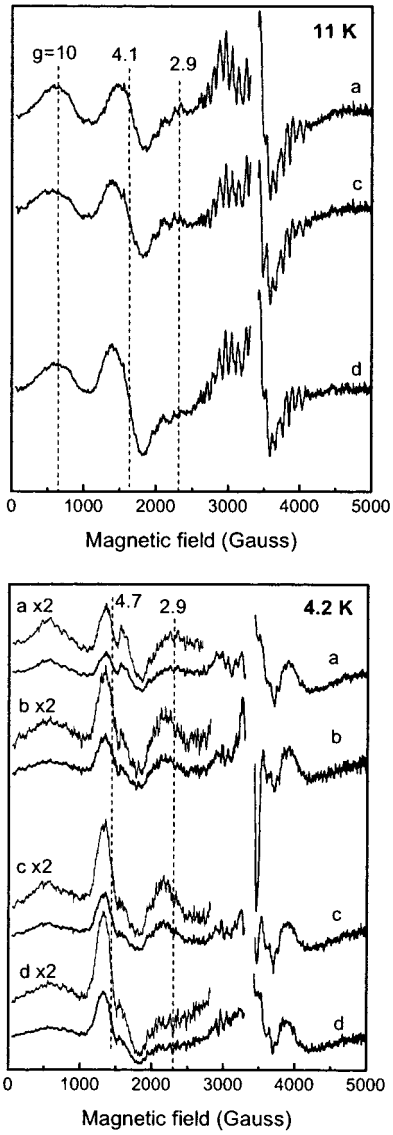

FIGURE 7: Induction of the $g = 5$ signal by excitation of the S_3 state with NIR light. Spectra were recorded after the following successive treatments of the same sample: (a) the S_3 state as prepared, (b) immediately after NIR excitation at 4.2 K, (c) 100 min incubation at 4.2 K and 30 min incubation at 11 K, and (d) 15 min incubation at 77 K. Difference spectra were obtained after subtraction of the dark adapted spectrum as described in the Materials and Methods section. EPR conditions: temperature as indicated in the panels, microwave frequency 9.39 GHz, microwave power 35 mW, modulation amplitude 25 G, modulation frequency 100 kHz.

Figure 7a shows the spectrum of the S_3 state as prepared. The sample was subsequently excited by NIR light at 4.2 K. This resulted in the parallel formation of the broadened $g \sim 2$ signal and the $g = 5$ signal with the 2.9 component (*19, 23*), Figure 7b. The spectrum recorded following a dark adaptation period at 4.2 and 11 K, which allowed for an approximately 70% decay of the $g = 2$ signal, is shown in Figure 7c. A small increase/sharpening of the $g = 5$ signal can be observed. Finally, the sample in c was transferred for 15 min at 77 K, and the new spectrum was recorded, Figure 7d. This resulted in the elimination of the $g = 2.9$ signal and a narrowing and increase of the $g = 5$ signal. These changes are more clearly seen in the spectra at 4.2 K. At 11 K, the $g = 5$ signal is obscured by the $g = 4.1$ signal

from the portion of centers in the S_2 state. The latter signal is partially saturated and thus makes a smaller contribution at 4.2 K. It should be noted that the NIR illumination had no effect on the amplitude of $Y_D^{\bullet}$.

In a recent communication (*23*), the $g = 5/2.9$ signals induced by NIR light, as well as the $g = 5$ signal that results from the slow decay of the S_3 state at 77 K, were assigned to the same $S = {}^7/_2$ configuration of the Mn cluster. Small changes in the crystal field parameters (reflecting structural changes), induced by the different treatments (NIR excitation vs incubation at 77 K), cause different relative amplitudes of the $g = 5$ and 2.9 features. While a more thorough analysis (see also *37*), including the orientation dependence of the signals is currently in progress, a number of qualitative remarks can be made on the spectra.

The nearly-isotropic "$g = 5$ only" spectrum, obtained after the prolonged incubation of the S_3 state at 77 K, Figures 1d and 6b, appears to represent the most relaxed configuration of the $S = {}^7/_2$ state. The $g = 5/2.9$ spectrum obtained by NIR-excitation appears to represent a transient configuration. The gradual conversion to the nearly isotropic form, e.g., spectra c and d of Figure 7, results in a sharpening and increase of the $g = 5$ component, but as can be verified by theory (*23*, *37*), the number of centers contributing to the spectra remains the same. This argues against the possibility that the increase in the $g = 5$ signal in spectrum c relative to spectrum b in Figure 7 is at the expense of the $g = 2$ radical. Spectrum b in this figure was recorded immediately after the NIR excitation, while spectrum c was recorded after the decay of the largest fraction of the radical. A close inspection of several experiments with varying NIR-excitation periods indicated that the $g = 5$ signal forms concomitantly to the $g = 2$ broad radical. What may accordingly affect the apparent intensity of the $g = 5$ signal is a change in the crystal field parameters in the presence and the absence of the radical species. It is possible, e.g., that during formation of the radical, proton shifts and Coulombic interactions cause small changes to the bond lengths/angles in the Mn cluster, resulting in a small and negative value of the *D* parameter of the empirical spin Hamiltonian (*23*). After decay of the radical, a slow rearrangement of the cluster occurs, which results in positive *D* values. An alternative interpretation could be that the magnetic interaction of the radical with the Mn cluster, which results in the broadening of the radical spectrum, broadens also the $g = 5/2.9$ spectrum. Preliminary theoretical simulations indicated, however, that a magnetic coupling that would produce a significant broadening of the radical signal would induce a nonobservable broadening in the $g = 5/2.9$ spectrum.

The $S = {}^7/_2$ configuration is assigned to a modified S_2 state (denoted S_2'), as was argued earlier in this paper. The rapid attainment by the NIR-light-excitation of the same modified S_2 configuration of the Mn cluster that results from the slow reduction of the S_3 state at 77 K is astonishing. It appears that the NIR-light excitation of the freshly prepared S_3 state accelerates charge recombination in some of the centers. Conceivably, this is possible if we assume that the NIR excitation causes the transfer of the positive hole from the Mn cluster to a nearby residue forming the broadened $g = 2$ radical. The radical species (tyr $Z^{\bullet}$, as argued in the following paper, *21*) in turn recombines rapidly with Q_A^- to yield an excited S_2 state configuration, S_2', identical to the one that evolves during the very slow recombination of S_3 with Q_A^- at 77 K. One would accordingly expect a small decrease in the intensity of the $Q_A^-Fe^{2+}$ signal accompanying the decay of the radical signal. As the inherently weak $Q_A^-Fe^{2+}$ signal in Figure 7a represents 100% of the centers while the radical species represents less than 10% of the PSII centers (*19*), such a decrease would be difficult to detect. Nevertheless, a small decrease can be discerned in the spectra c and d of Figure 7. Aletrnatively, in preliminary experiments using the exogenous electron acceptor phenyl-p-benzoquinone (*38*), the NIR-induced radical species was very stable over a period of 4 h at 11 K in the absence of Q_A^- (data not shown).

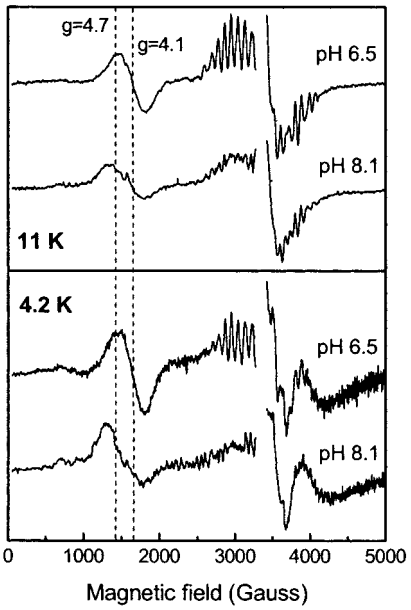

FIGURE 8: S_2 state spectra at alkaline pH contain a $g = 5$ contribution. The same sample was incubated first at pH 6.5 and subsequently at pH 8.1 (see Materials and Methods). The S_2 state was produced by illumination of the S_1 state at −30 °C in the presence of the atrazine inhibitor. Difference spectra were obtained by subtraction of the respective S_1 traces at each pH. EPR settings were the same as those in Figure 4. Recording temperatures as indicated.

S_2 State Spectra at Alkaline pH Contain a $g = 5$ Contribution. It was shown in the preceding experiments that incubation at 77 K or NIR excitation of the S_3 state at 4.2 K invariably result in the decay of S_3 to S_2'. The latter is a modified S_2 configuration, most likely deficient by one proton, as originally suggested (*22*). The relaxation of S_2' to the normal S_2 configuration at −50 °C and higher temperatures is accordingly attributed to protonation of the Mn cluster (not excluding parallel conformational changes).

The above interpretation is supported by experiments, which show that production of the S_2 state by the straightforward illumination of S_1 at −30 °C at alkaline pH is accompanied by the formation of a $g = 5$ signal. An experiment performed as described in the Materials and Methods section is depicted in Figure 8. This compares the S_2 state spectra of the same sample at pH 6.5 and 8.1. The intensity of the S_2 state signals (multiline and $g = 4.1$) is greatly reduced on going from pH 6.5 to 8.1. Notable is, however, the formation of a $g = 5$ signal at pH 8.1.

The decrease of the multiline signal at high pH is compatible with the systematic observations of Geijer et al.

(*39*), but as these authors used 5% methanol, which is known to enhance the S_2 multiline signal at the expense of alternative signals, no comparison can be made with the changes in the low-field EPR signals of Figure 8. Geijer et al. (*39*) attributed the diminution of the multiline signal at high pH to protonation/deprotonation of ligands to the Mn (other possibilities were considered as well). This agrees with the present observations. Actually, the fact that the same $g = 5$ conformation appears to be trapped during the decay of S_3 at 77 K (or even at 4.2 K by the NIR excitation) as well as during the light-induced advancement of the S_1 to S_2 state at alkaline pH suggests deprotonation of the same Mn ligand in both cases. Clearly, the high-pH effects deserve a more systematic study before final conclusions can be made.

The NIR excitation of the S_3 state at liquid-helium temperatures, produces excited-S_3-state transients in addition to the $g = 5/2.9$ signal (*19*). These, as well as the products of the light excitation of the S_2' state, are studied in the companion paper (*21*). The overall phenomenology is examined in the context of a molecular model, which provides useful insights into the interrelation of the Mn cluster and tyr Z.

ACKNOWLEDGMENT

We thank Dr. J. Nugent for helpful discussions and Mr. P. Tampourlos for technical help. N.I. thanks I.K.Y. (Greek State Scholarship Foundation) for financial support.

REFERENCES

1. Britt, R. D. (1996) *Advances in Photosynthesis: Vol. 4 Oxygenic Photosynthesis: The Light Reactions* (Ort, R. D., and Yocum, C. F., Eds) pp 137−164, Kluwer Academic Publishers, Dordrecht, The Netherlands.
2. Diner, B. A. and Babcock, G. T. (1996) *Advances in Photosynthesis: Vol. 4 Oxygenic Photosynthesis: The Light Reactions* (Ort, R. D., and Yocum, C. F., Eds) pp 213−247, Kluwer Academic Publishers, Dordrecht, The Netherlands.
3. Rutherford, A. W. (1989) *Trends Biol. Sci. 14*, 227−232.
4. Debus, R. J. (1992) *Biochim. Biophys. Acta 1102*, 269−352.
5. Bricker, T. M.; Ghanotakis, D. F. (1996) *Advances in Photosynthesis: Vol. 4 Oxygenic Photosynthesis: The Light Reactions* (Ort, R. D., and Yocum, C. F., Eds) pp 113−136, Kluwer Academic Publishers, Dordrecht, The Netherlands.
6. Yachandra, V. K., Sauer, K., and Klein, M. P. (1996) *Chem. Rev. 96*, 2927−2950.
7. Messinger, J., Nugent, J. H. A., and Evans, M. C. W (1997) *Biochemistry 36*, 11055−11060.
8. Åhrling, K. A., Peterson, S., and Styring, S. (1997) *Biochemistry 36*, 13148−13152.
9. Messinger, J., Robblee, J. H., Wa On Yu, Sauer, K., Yachandra, V. K., and Klein, M. P. (1997) *J. Am. Chem. Soc. 119*, 11349−11350.
10. Dexheimer, S. L., and Klein, M. P. (1992) *J. Am. Chem. Soc. 114*, 2821−2826.
11. Yamauchi, T., Mino, H., Matsukawa, T., Kawamori, A., and Ono, T. (1997) *Biochemistry 36*, 7520−7526.
12. Campbell, K. A., Gregor, W., Pham, D. P., Peloquin, J. M., Debus, R. J., and Britt, R. D. (1998) *Biochemistry 37*, 5039−5045.
13. Dismukes, G. C., and Siderer, Y. (1981) *Proc. Natl. Acad. Sci. U.S.A. 78*, 274−278.
14. Casey, J. L., and Sauer, K. (1984) *Biochim. Biophys. Acta 767*, 21−28.
15. Zimmermann, J. L., and Rutherford, A. W. (1984) *Biochim. Biophys. Acta 767*, 160−167.
16. Boussac, A., Girerd, J.-J, and Rutherford, A. W. (1996) *Biochemistry 35*, 6984−6989.
17. Boussac, A., Un, S., Horner, O., and Rutherford, A. W. (1998) *Biochemistry 37*, 4001−4007.
18. Matsukawa, T., Mino, H., Yoneda, D., Kawamori, A. (1999) *Biochemistry 38*, 4072−4077.
19. Ioannidis, N., and Petrouleas, V. (2000) *Biochemistry 39*, 5246−5254.
20. Boussac, A., Sugiura, M., Inoue, Y., and Rutherford, A. W. (2000) *Biochemistry 39*, 13788−13799.
21. Ioannidis, N., Nugent, J. H. A., and Petrouleas, V. (2002) *Biochemistry 41*, 9589−9600.
22. Nugent, J. H. A., Turconi, S., and Evans, M. C. W. (1997) *Biochemistry 36*, 7086−7096.
23. Sanakis, Y., Ioannidis, N., Sioros, G., and Petrouleas, V. (2001) *J. Am. Chem. Soc. 123*, 10766−10767.
24. Berthold, D. A., Babcock, G. T., and Yocum, C. F. (1981) *FEBS Lett. 134*, 231−234.
25. Ford R. C., and Evans, M. C. W. (1983) *FEBS Lett. 160*, 159−164.
26. Vass, I., Deak, Z., and Hideg, E. (1990) *Biochim. Biophys. Acta 1017*, 63−69.
27. Buser, C., and Brudvig, G. W. (1992) *Research in Photosynthesis* (Murata, N., Ed.) Vol II pp85−88, Kluwer Academic Publishers, Dordrecht, The Netherlands.
28. Nugent, J. H. A., Demetriou, C., and Lockett, C. (1987) *Biochim. Biophys. Acta 894*, 534−542.
29. Diner, B. A. (2000) *Biochim. Biophys. Acta 1503*, 147−163.
30. Styring, S. A., and Rutherford, A. W. (1987) *Biochemistry 26*, 2401−2405.
31. Kawamori, A., Satoh, J., Inui, T., and Satoh, K. (1987) *FEBS Lett. 217*, 134−138.
32. Pace, R. J., Smith, P., Bramley, R., Stehlik, D. (1991) *Biochim. Biophys. Acta 1058*, 161−170.
33. Lavergne, J., and Etienne, A. L. (1980) *Biochim. Biophys. Acta 593*, 136−148.
34. Sane, P. V., Rutherford, A. W. (1986) *Light Emission by Plants and Bacteria* (Govindjee, Amesz, J., and Fork, D. C. Eds.) pp 329−360, Academic Press Inc, New York.
35. Demeter, S., Goussias, Ch., Bernat, G., Kovacs, L., Petrouleas, V. (1993) *FEBS Lett. 336*, 352−356.
36. Kanazawa, A., Kramer, D., Crofts, A. (1992) in *Research in Photosynthesis Vol II* (Murata, N., Ed.) pp 131−134, Kluwer Academic Publishers, Dordrecht, The Netherlands.
37. Ioannidis, N., Sanakis, Y., Sioros, G., and Petrouleas, V. (2001) in *Proceedings of the 12th International Congress on Photosynthesis*, CSIRO Publishing, Collingwood, Australia (www.publish.csiro.au/ps2001; ISBN 0643 067116).
38. Petrouleas, V., and Diner, B. A. (1987) *Biochim. Biophys. Acta 893*, 126−137.
39. Geijer, P., Deak, Z., and Styring, S. (2000) *Biochemistry 39*, 6763−6772.

BI0159938